

Design and Fabrication of a Triple Band Microstrip Antenna for WLAN, Satellite TV and Radar Applications

Prem P. Singh* and Sudhir K. Sharma

Abstract—A compact and hexagon-shaped microstrip patch antenna operating in three bands is described in this paper. Multiband functionality of the antenna is achieved by adding two inclined strips and cutting modified slots on the radiating patch. The antenna consists of a hexagonal patch and partial ground plane, has the total dimensions of $15 \times 17 \times 1.6 \text{ mm}^3$, and operates over three frequencies 5.40 GHz, 6.76 GHz, and 8.82 GHz for WLAN, TV satellite broadcasting, WiMAX (5250–5850 MHz), IEEE 802.11a (5.47–5.725 GHz), 5G Unlicensed band (5.2–5.7 GHz), weather monitoring, and radar applications. This antenna has the novelty that it can also be used as a reconfigurable antenna, and the notched bands can be controlled. Simulation of the proposed antenna is carried out using HFSS-15 software. To verify the simulated results, and a prototype of the proposed antenna is fabricated. After measurement, simulated and measured results are in good agreement.

1. INTRODUCTION

The demand for compact and multiband antennas is increasing to raise technology development. Multiband antennas are useful to utilize the frequency spectrum. In present wireless communication system, there is always a need of an antenna which can cover multiple wireless services [1]. Various approaches have been used to design multiband antennas in the literature. In cognitive and multiservice radios, multiband antenna plays an important role. In addition, incorporating multiple bands into a single antenna becomes essential and in various wireless services.

In [2], a triple band antenna with a pentagon-shaped patch and partial ground plane is proposed. To generate multiple bands, a slot and two hook-shaped resonators are connected to upper side of the patch. The antenna is useful for three applications, WiMAX, WLAN, and X-Band uplink satellite communication. A rectangular meandered strips connected antenna for multiband operation is presented in [3]. An FR-4 substrate with the overall size of $40 \times 32 \text{ mm}^2$ and thickness $h = 1.6 \text{ mm}$ is used to print the antenna, and the operating frequencies are 4.27 GHz, 4.85 GHz, and 6.45 GHz. Another antenna for simultaneous multiple applications is proposed by Pandya et al. [4]. An FR-4 substrate (Dielectric Constant = 4.4) is used for the fabrication of the antenna and useful for WLAN, WiMax, and Wi-Fi services. In this antenna, the ground plane is modified with five different Split Ring Resonators (SRRs). Dimension of the antenna is $83 \times 56 \text{ mm}^2$, and it resonates at 2.47 GHz, 3.55 GHz, and 5.55 GHz. Gain provided by the antenna is about uniform on all the operating frequencies, and the maximum gain is 3.88 dBi. Since any communication system may operate in different frequency bands, instead of use of multiple antennas it is useful to have a single antenna for several communication services. Slot plays a crucial role in the size reduction of an antenna for dual-band operation. A multiband frequency reconfigurable antenna is reported in [5]. The antenna has a rectangular patch and a ground plane which is modified using DGS (Defected ground structure). The overall antenna dimension is $47 \times 37 \text{ mm}^2$.

Received 13 December 2021, Accepted 7 January 2022, Scheduled 11 January 2022

* Corresponding author: Prem Pal Singh (ppsherpur.12392@gmail.com).

The authors are with the Department of Electronics and Communication Engineering, Jaipur National University, Jaipur, India.

Multiband antennas are very efficient in wireless communication system for signal broadcasting. In [6], a triple band antenna is designed having high gain with modified ground plane fed with coaxial feed. Operating frequency range of the antenna is 4–6 GHz. Similarly, a slotted multiband antenna is proposed in [7] by Yu et al. The proposed design resonates on four different frequencies which are 1.6 GHz (1.58–1.77) GHz, 2.35 GHz (2.1–2.50 GHz), 3.8 GHz (3.61–4.09 GHz), and 5.85 GHz (4.75–6.5 GHz) with sufficient bandwidth of more than 12%. Overall substrate size of the antenna is $85 \times 70 \text{ mm}^2$. The patch of the antenna is circular shaped with a “回” structure looking like an ancient Chinese window grille etched on FR-4 having ϵ_r of 4.4.

The antenna printed on a rectangle-shaped substrate with differently shaped patches connected to each other. Substrate has the size of $46 \times 50 \text{ mm}^2$, and the antenna is fed with microstrip feed line. The proposed antenna in [8] uses two stacked patches to operate the antenna for dual bands. Other multiband antennas with DGS, U-slot on patch, cascaded E-type unit cell defected ground structure are proposed in [9–11]. A linearly polarized antenna operating over four frequencies 0.82, 2.42, and 3.2 and 5.72 GHz excited with CPW feed is presented by Bashir et al. in [12] for LTE-4G, TV broadcasting, and 5G applications. The antenna consists of a truncated octahedron with a substrate size of $190 \times 90 \text{ mm}^2$. Bandwidth of the antenna for all bands is more than 300 MHz. The effect of surrounding metal objects on the antenna performance is also studied, and it shows that the metal objects near the antenna have both positive and negative effects. A CPW-fed antenna for WLAN and WiMax bands with the substrate dimensions of $24 \times 21 \text{ mm}$ is reported in [13]. Antenna comprises a trapezium shaped patch with a V-slot and two inverted L-shaped slots inserted in the patch. The gain provided by the antenna in the lower band of 2.4 GHz is lower due to low efficiency.

In this paper, a hexagon-shaped antenna with two inclined strips connected to the patch is presented. The proposed antenna operates on three different frequencies with sufficient gain over all three bands and also has a compact size of $15 \times 17 \text{ mm}^2$.

2. ANTENNA DESIGN

Geometry of the antenna is depicted in Figure 1. As shown in the figure the main radiating part of the antenna consists of a hexagon-shaped patch fed with a 50 ohm microstrip line.

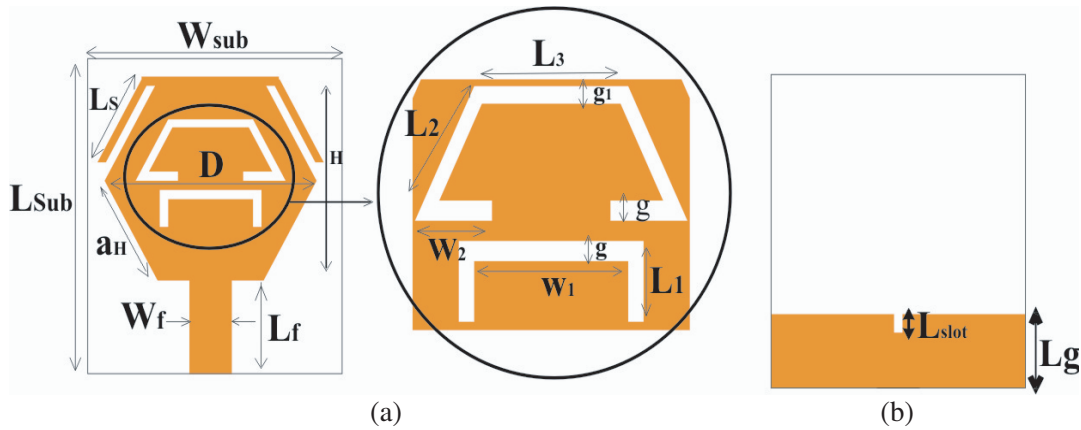


Figure 1. Geometry of the antenna. (a) Patch side. (b) Ground plane.

The proposed hexagonal patch can be obtained as shown in Figure 1(a). Side length a_H of the hexagonal patch can be found using the following equation [14] for initial resonant frequency (f_r) of 5.7 GHz

$$a_H \frac{F}{\left\{ \left[1 + \left(\frac{2h}{\pi \epsilon_r F} \right) \right] \left[\ln \left(\frac{nF}{2h} + 1.7726 \right) \right] \right\}^{0.5}} \quad (1)$$

where

$$F = \frac{8.791 \times 10^9}{f_r \sqrt{\epsilon_r}}$$

h is the height of the substrate, and n is the number of sides and in this work $n = 6$.

a_H obtained is equal to 6.28 mm, and practically the value of a_H selected is 6.25 mm given in Table 1.

Table 1. Dimensional parameters of the antenna.

Parameter	Value (mm)	Parameter	Value (mm)
L_{Sub}	17	L_1	2
W_{Sub}	15	L_2	4
L_S	5	L_3	5
L_f	5	W_1	6
W_f	2.5	W_2	2.5
L_g	4	$g = L_{slot}$	0.5
D	12.5	g_1	0.6
a_H	6.25	H	10.80

The diameter (D) of the hexagonal patch is given by

$$D = 2 \times a_H \tag{2}$$

Height of the hexagonal patch (H) is

$$H = \sqrt{3}a_H \tag{3}$$

$$H = \sqrt{3} \times 6.25 = 10.82 \text{ mm}$$

The value of the H obtained from the equation is 10.82 mm, and the selected value is 10.8 mm.

Ground plane is a partial ground with a slot inserted at the upper side of the ground of size $1 \times 0.5 \text{ mm}^2$. Two inclined strips are connected to the patch in the upper side. Also the patch is modified with two slots. Dimensions of the antenna are listed in Table 1.

An iterative design process for the antenna has been used which is shown in Figure 4. In the first step, a hexagon-shaped antenna is designed and excited with a microstrip line of length L_f and width W_f . The antenna operates over a wide frequency range of 6.00–12.42 GHz, and the input impedance varies between 50Ω and 60Ω for the entire range of operation in step 1.

As a CSRR and inverted-U slot etched on the patch and two inclined stubs are added to the patch, the equivalent circuit of the proposed antenna is illustrated in Figure 2. Resistance (R), capacitance (C), and inductance (L) are used to draw the equivalent circuit of the proposed antenna. Three parallel resonant circuits are drawn as antenna resonates on three frequencies. Simulated return loss parameters and VSWR are illustrated in Figures 3(a) and 3(b). As can be seen in Figure 3(a), the antenna operates over three different frequencies (5.38, 6.76, and 8.82 GHz), and the corresponding values of VSWR are in the range, i.e., $VSWR < 2$ for all operating frequencies.

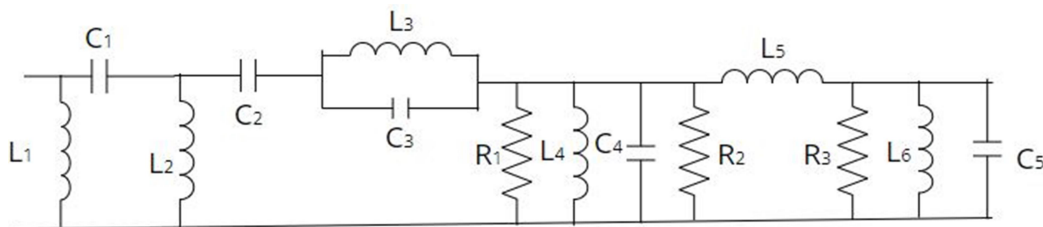


Figure 2. Equivalent circuit of the antenna.

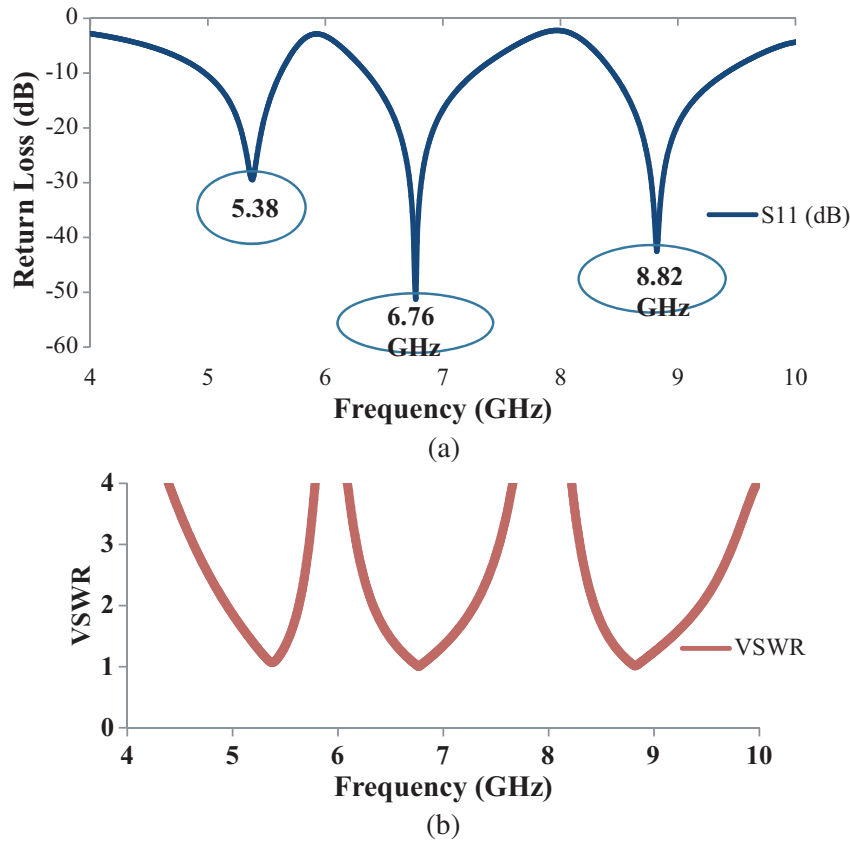


Figure 3. Simulated results of the proposed antenna. (a) Return loss parameters. (b) VSWR.

In the second step, i.e., iteration 2, two inclined strips are connected to the upper side of the radiating patch, and also a trapezium shaped slot and a small rectangular slot of 1×0.5 mm are etched in the ground for matching purpose. The lower slot is an inverted U-slot, and the other is a modified trapezium shaped slot shown in the figure encircled in Figure 1(a) and is etched after this antenna operates for three bands as depicted in Table 2 for 5.09–5.72 GHz, 6.89–7.69 GHz, and 8.34–12.60 GHz. Due to the connected strips, the electrical length of the radiating part changes. Also it helps to convert the antenna as a triple band antenna. The antenna obtained in iteration-2 can also be used as an individual antenna for frequency range of 5 to 12.5 GHz with two notch bands, but our aim is to design an antenna for triple band operation.

For this an inverted U-slot is inserted in the next iteration, i.e., in iteration-3. This change made in iteration-3 results in an antenna which operates over three different frequencies shown in Table 2. The antenna resonates at three frequencies 5.38, 6.76, and 8.82 GHz. -10 dB bandwidths of 610 MHz, 900 MHz, and 930 MHz are obtained for the first, second, and third operating bands, respectively, as shown in Figure 5.

Table 2. Operating frequency ranges for three iterations.

Iteration No.	Frequency Bands (GHz)
Iteration 1	6.00–12.42
Iteration 2	5.09–5.72, 6.89–7.69, 8.34–12.60
Iteration 3	5.00–5.61, 6.36–7.26, 8.46–9.39

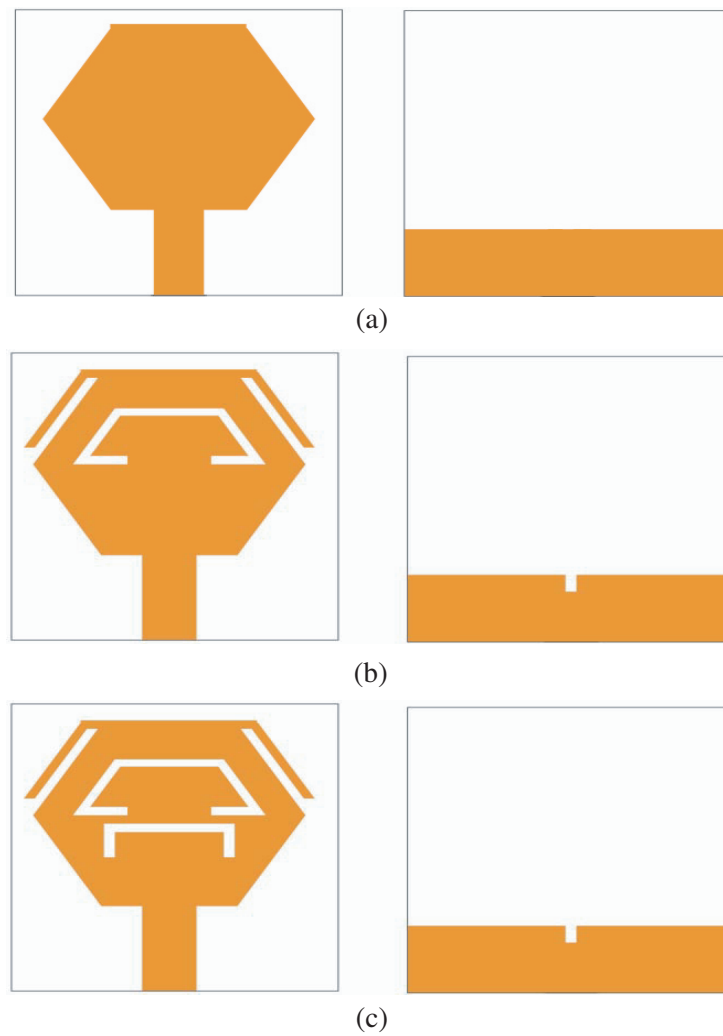


Figure 4. Design iterations of the antenna. (a) Iteration-1. (b) Iteration-2. (c) Iteration-3.

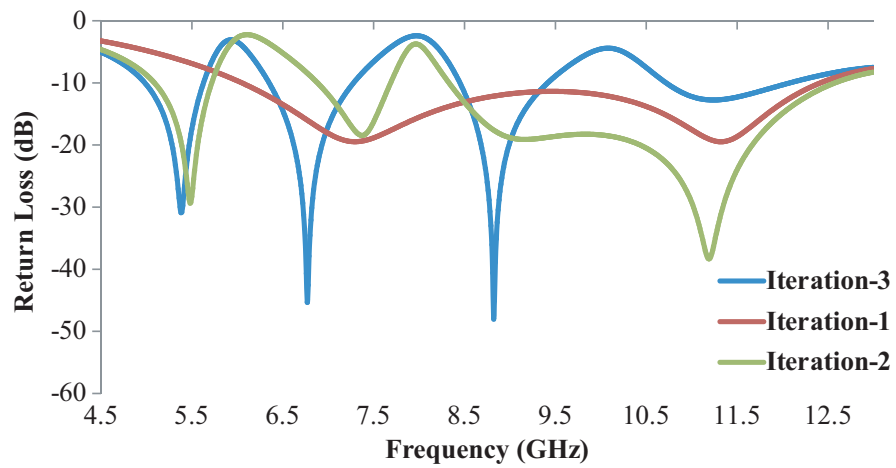


Figure 5. Reflection coefficient comparison of each iteration.

2.1. Parametric Analysis

The effect of the variation in parameter L_s on the return loss characteristics is illustrated in Figure 6(a). It is clear from surface current distribution shown in Figure 7(c) that L_s is responsible for higher band, i.e., the third band, so as shown in Figure 6(a) it can be observed that varying L_s , upper resonating frequency shifts towards right, i.e., towards higher frequency. L_s varies as 2, 3, and 5 mm. Effect of L_s on the two lower bands is negligible. Figure 6(b) illustrates the impact of varying W_2 on the return loss parameters. Variation in W_2 shifts the middle band of 6.76 GHz towards right side. Also the first band shifts towards higher frequency while the third band is resistive toward any variation in W_2 . So by varying the length L_s and slot length W_2 , operating frequencies can be adjusted.

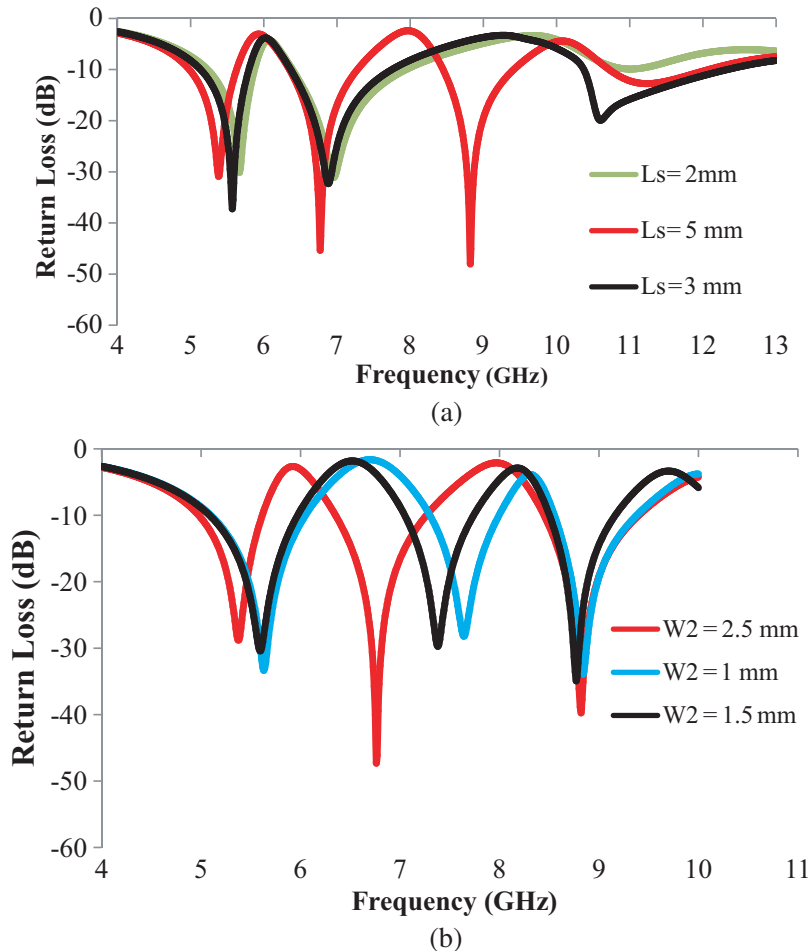


Figure 6. Reflection coefficient of the antenna against varying parameters. (a) L_s . (b) W_2 .

So it is clear that L_s does not affect the lower operating bands, and it only affects the third band while W_2 affects only the first and second bands, and it does not have any effect on the third band, so three bands can be controlled easily. This has been described in the Section 2.1 that L_s and W_2 are responsible for the particular bands.

2.2. Surface Current Distribution

Surface current distribution of the designed antenna is shown in Figure 7 for three operating frequencies 5.38, 6.76, and 8.82 GHz. Figure 7(a) illustrates the current distribution for 5.38 GHz, and it can be observed that most of the current is distributed over the lower side of the trapezium-shaped slot, and

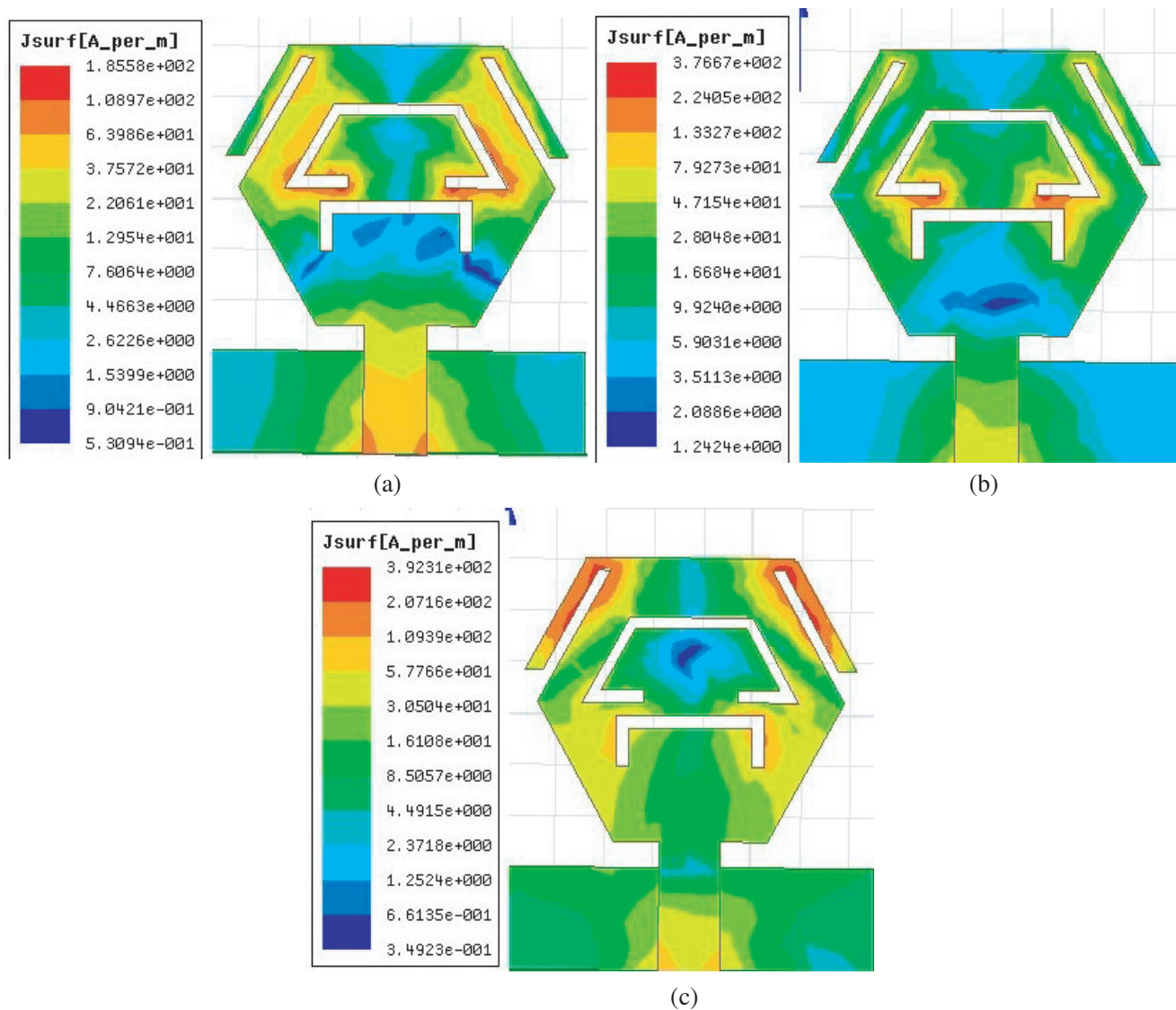


Figure 7. Surface current distribution. (a) 5.38 GHz. (b) 6.76 GHz. (c) 8.82 GHz.

some of the current is also distributed on the upper left/right part of the hexagon-shaped radiating patch. The current distribution for frequency 6.76 GHz is shown in Figure 7(b). After observing this figure we can say that the current is distributed on the lower side of the trapezium slot. Thus, the frequency can be adjusted or controlled by the variation of the length W_2 . Current on the bottom side of antenna is uniformly distributed. Similarly, Figure 7(c) shows the current distribution for 8.82 GHz. It is clear from the figure that the current is distributed on the inclined strips. Thus by varying the length L_S , operating frequency can be controlled.

Performance analysis of the antenna is done in terms of S_{11} by varying parameters in this section. Figure 6 shows the effect of different parameters (L_s and W_2) on the reflection coefficients (S_{11}).

3. RESULTS AND DISCUSSIONS

To verify the performance and results of the simulated antenna, a prototype is fabricated. An FR-4 substrate having ϵ_r 4.4 and thickness 1.6 mm is used. Vector network analyzer (VNA) is used to measure the reflection coefficients. The antenna is excited with a commercially available $50\ \Omega$ SMA connector.

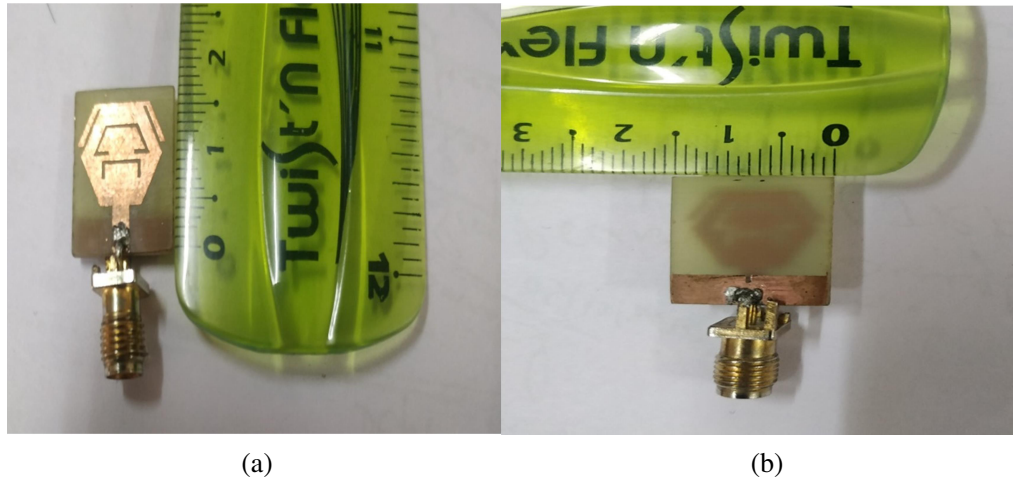


Figure 8. Fabricated prototype of the antenna. (a) Front view. (b) Bottom view.

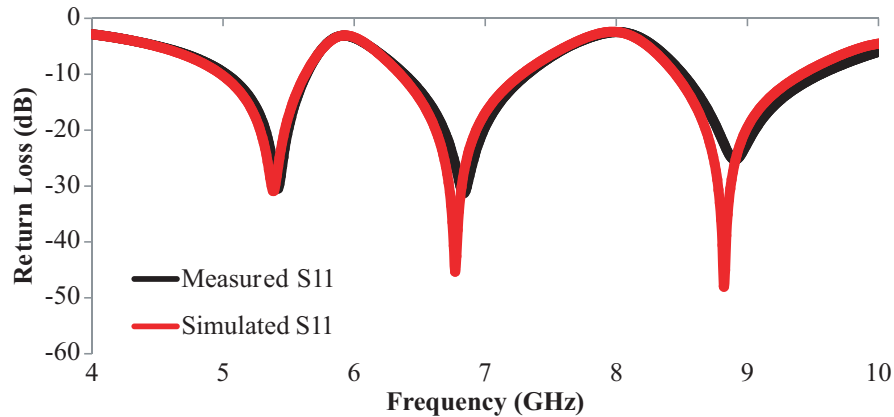


Figure 9. Simulated and measured return loss comparison.

The fabricated prototype of the proposed antenna is presented in Figure 8, and Figure 9 shows the simulated and measured reflection coefficients for the fabricated antenna. A good agreement between simulated and measured results is obtained, and it can be noted that simulated and measured S_{11} parameters cover the desired operating bands. Table 3 shows the summary of simulated and measured return loss values and operating frequencies.

There is a small difference between measured and simulated return loss parameters which is due to the fabrication and soldering tolerance.

In Figure 10, the 3D plots of gain of the antenna for three operating bands are depicted. The gain for 5.38 GHz is 2.42 dBi. The gains over the other two bands (6.76 and 8.82 GHz) are 2.46 and 4.28 GHz,

Table 3. Summarized simulated and measured results.

Operating Frequency (GHz)		Return Loss (S_{11}) (dB)		Gain (dBi)
Simulated	Measured	Simulated	Measured	
5.38	5.42	-30.88	-30.46	2.42
6.76	6.84	-45.32	-31.25	2.46
8.82	8.93	-47.93	-25.03	4.28

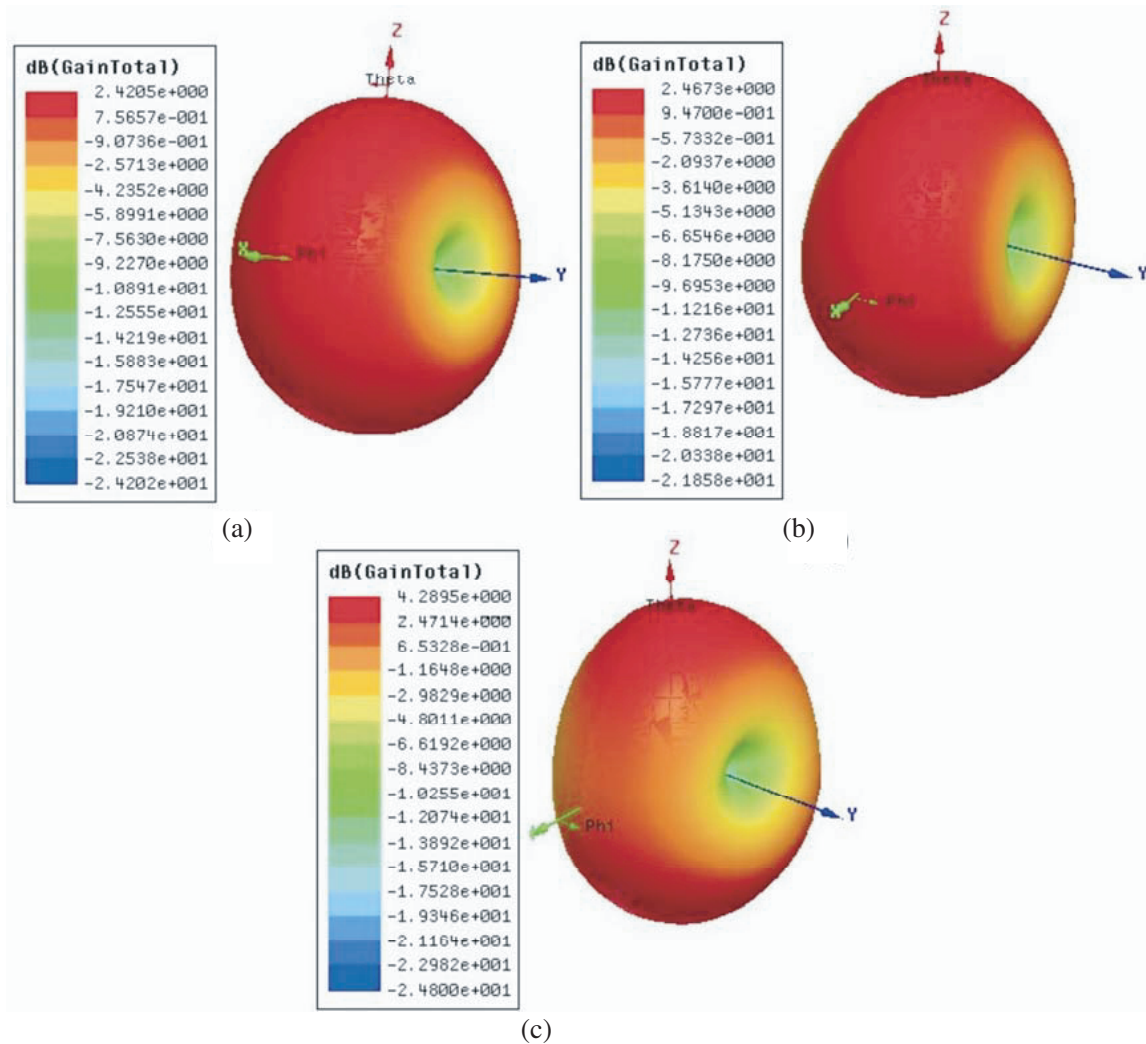


Figure 10. Gain of the antenna. (a) 5.38 GHz. (b) 6.76 GHz. (c) 8.82 GHz.

respectively.

Simulated and measured 2D radiation patterns for both planes (E - and H -planes) are depicted in Figure 11 for three resonant frequencies. At 5.76 and 8.82 GHz, the antenna radiates as a ‘figure of eight’ in elevation plane and azimuth plane, and at 6.76 GHz main lobe of the antenna is directed towards 180° in the E -plane and radiates as ‘figure of eight’ in H -plane.

3.1. Reconfigurability Function of the Antenna

The proposed antenna is able to operate over three bands, and these bands can be controlled. Thus, the antenna acts as a multiband reconfigurable antenna, or it covers the frequency range from 5.00 GHz to 12.38 GHz. Therefore, the antenna can be operated with multiband reconfiguration. Two side strips of length L_s are responsible for the third band of the antenna. These two inclined strips can be connected or disconnected using PIN diodes, and these PIN diodes can be simulated in HFSS using lumped element as the equivalent circuit of PIN diode comprising resistor, capacitor, and inductor in ON and OFF states. Two PIN diodes are used in the upper side of the patch to connect/disconnect inclined strips, and another PIN diode is used in lower inverted U-slot. A capacitor is also used to isolate the RF current from mixing with DC supply which is indicated in diagram below in Figure 12.

PIN diode model used in this antenna is MA4AGBLP912 from M/A-COM company for simulation

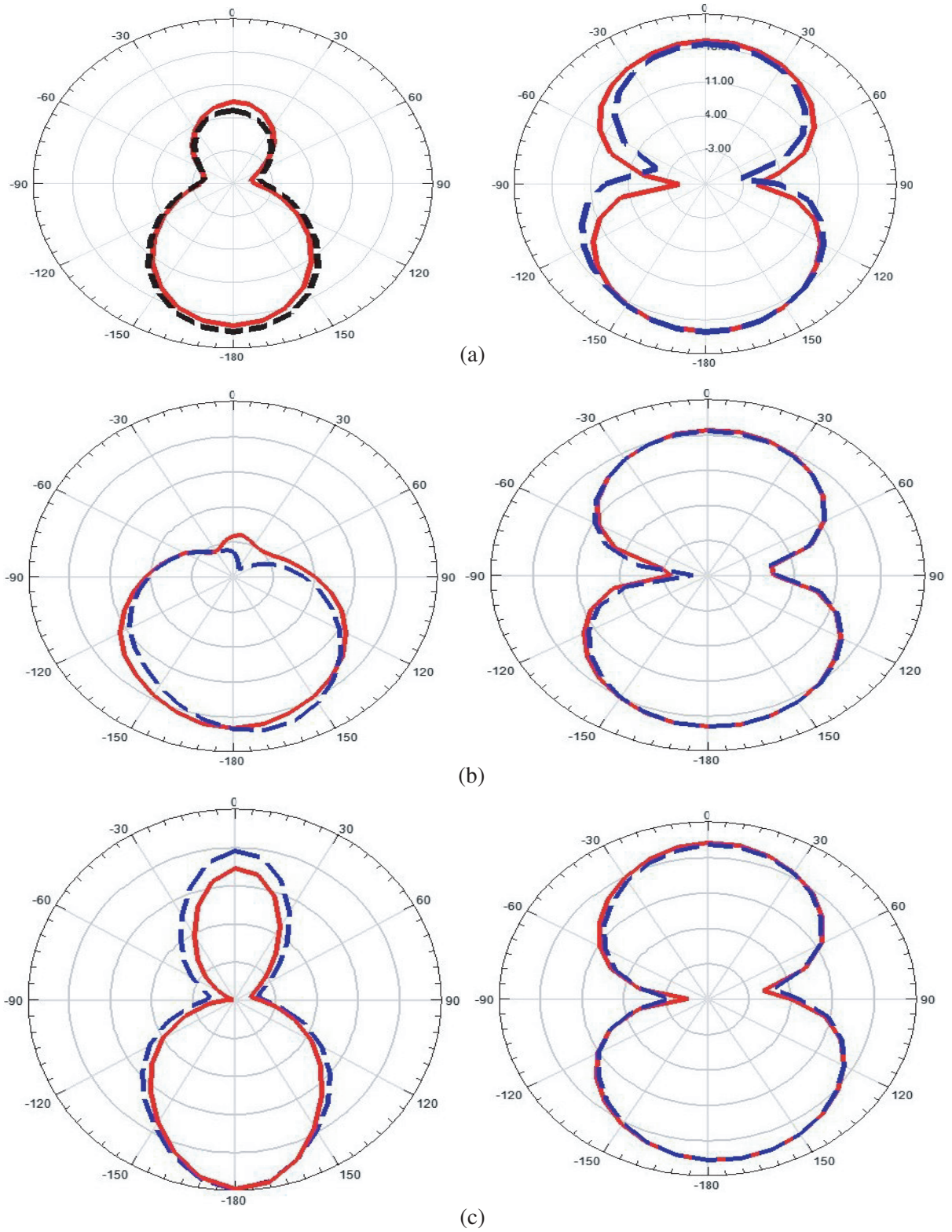


Figure 11. Simulated (solid line) and measured (dashed line) radiation pattern at (a) 5.38 GHz, (b) 6.76 GHz, (c) 8.82 GHz.

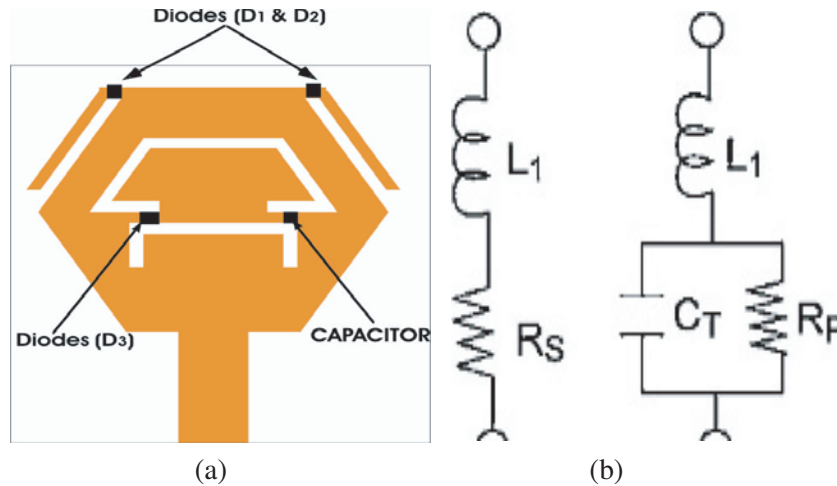


Figure 12. Reconfiguration mode of the antenna. (a) Reconfigurable antenna. (b) Equivalent circuit of pin diode in ON and OFF state.

purpose, and its equivalent circuit was simulated in HFSS with an inductor L_1 (0.5 nH) in series with a resistor R_S (4Ω) in forward condition and a parallel combination of a capacitor C_T (0.026 pF) and resistor R_P ($10 \text{ K}\Omega$) with an inductor L_1 (0.5 nH) in series in reverse condition.

In reconfigurable mode, the two upper PIN diodes are turned ON and OFF simultaneously. Thus, total four modes are possible. The simulated return loss parameters of the reconfigurable mode of the antenna are shown in Figure 13. The operating modes of the antenna are shown in Table 4.

From Figure 13 it is clearly observed that the proposed antenna can also be used in band reconfigurable mode. The antenna operates in dual band or triple band mode for different configurations of PIN diodes over C- and X-bands.

Table 4. Operating modes of the diodes.

Mode No.	State of Diode D_1 and D_2	State of Diode D_3
Mode-1	OFF	OFF
Mode-2	OFF	ON
Mode-3	ON	OFF
Mode-4	ON	ON

Table 5. Comparison of antenna with antennas studied in the literature.

Ref. No.	Size (mm^2)	O.F. (GHz)	BW (MHz)	Gain (dBi)
[2]	35×18	3.5, 5.4, 8	900, 800, 1600	3.66, 4.2, 4.00
[3]	40×32	4.27, 4.85, 6.45	120, 160, 250	1.76, 2.3, 1.45
[4]	83×56	2.47, 3.55, 5.55	380, 190, 300	3.88, 3.87, and 3.83
[6]	47×37	4.11, 4.47, 4.86, 5.80	190, 510, 90, 110	6.41 (Peak)
[9]	21×16	1.8, 2.4, 5.00	250, 50, 225	1.7, 2.4, 6.00
[11]	18×18	2.55, 3.47, 5.75	170, 100, 260,	0.2, 0.16, 0.62
[12]	130×90	2.42, 3.26, 5.78	294, 120, 310	2.76, 3.29, 5.96
Proposed Work	17×15	5.38, 6.76, 8.82	610, 900, 910	2.42, 2.46, 4.28

* O.F. = Operating Frequency, BW = Bandwidth.

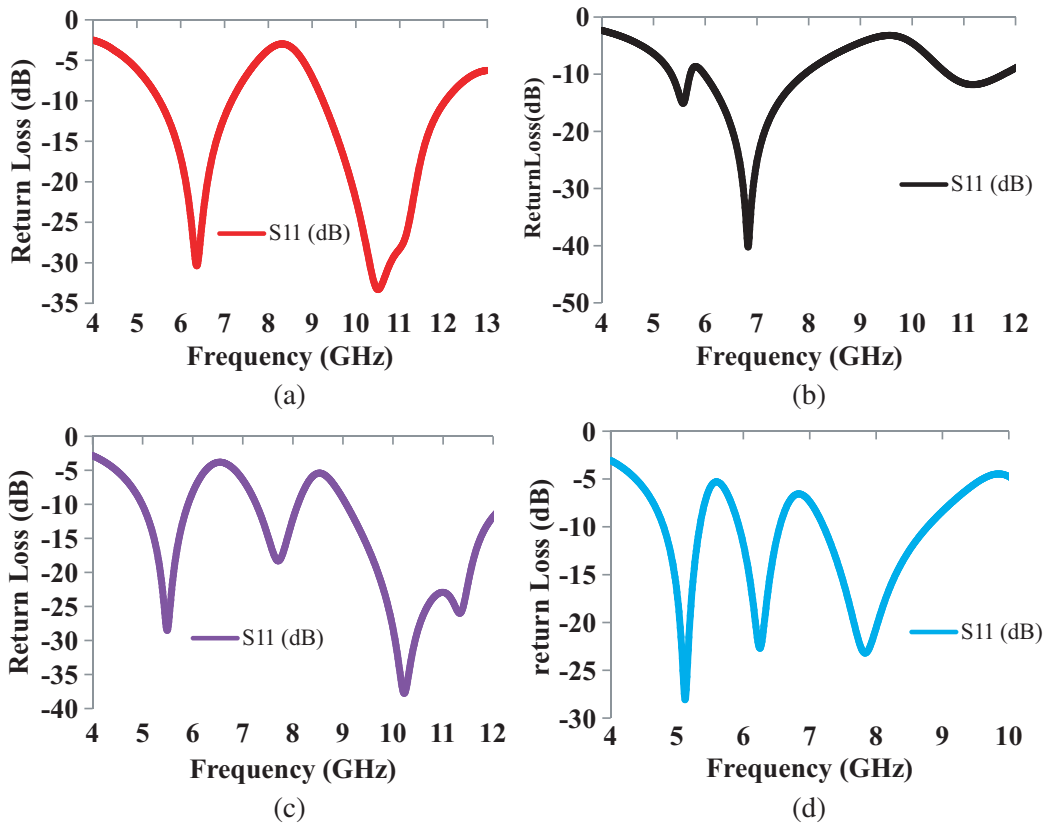


Figure 13. Reconfigurable modes of the proposed antenna. (a) Mode-1. (b) Mode-2. (c) Mode-3. (d) Mode-4.

The fabricated triple band antenna is compared with the previous designed antennas and shown in Table 5. Antennas are compared based on overall size, resonant frequencies, bandwidth, and gain obtained. It is clear from the table that the proposed antenna in this paper is compact in size and has sufficient bandwidth as compared to all the other designs given in Table 5. Apart from this, the proposed antenna has a sufficient gain.

4. CONCLUSION

A small size antenna for triple band operation for WLAN, satellite TV-broadcasting, weather monitoring, air traffic control, radar applications, unlicensed 5G, and many more in the frequency range of C and X bands is presented in this work. Three operating frequencies of 5.38, 6.76, and 8.82 GHz and sufficient gains of 2.42, 2.46, and 4.28 dBi are respectively obtained in this research work. With the variation in the two parameters (L_s , W_2), the antenna can be tuned for a particular frequency. Bandwidth for all three bands is more than 900 MHz. Hardware of the simulated antenna is fabricated, and results are measured successfully. The antenna is compared with some recently designed antennas, and it is clear from Table 5 that the presented antenna is compact and has wide bandwidth and high gain over all the bands. An additional advantage of this antenna is that the operating bands can be controlled by the associated parameters. Also the antenna was simulated in multiband reconfigurable mode in which the operating band of the antenna can be adjusted or reconfigured with the use of PIN diodes. In future, the number of operating bands can be increased, and antenna can be reconfigured with IoT devices having small size, gain, and efficiency.

ACKNOWLEDGMENT

I would like to thank Rajasthan University to provide testing facility and Jaipur National University to conduct research on this work.

REFERENCES

1. Singh, A. K., M. P. Abegaonkar, and S. K. Koul, "Miniaturized multiband microstrip patch antenna using metamaterial loading for wireless application," *Progress In Electromagnetics Research C*, Vol. 83, 71–82, 2018.
2. Mallat, N. K. and A. Iqbal, "Multi-band printed antenna for portable wireless communication applications," *Progress In Electromagnetics Research Letters*, Vol. 84, 39–46, 2019.
3. Iqbal, A., A. Bouazizi, O. A. Saraereh, A. Basir, and R. K. Gangwar, "Design of multiple band, meandered strips connected patch antenna," *Progress In Electromagnetics Research Letters*, Vol. 79, 51–57, 2018.
4. Pandya, A., T. K. Upadhyaya, and K. Pandya, "Tri-band defected ground plane based planar monopole antenna for Wi-Fi/WiMAX /WLAN applications," *Progress In Electromagnetics Research C*, Vol. 108, 127–136, 2021.
5. Jenath Sathikbasha, M. and V. Nagarajan, "DGS based multiband frequency reconfigurable antenna for wireless applications," *International Conference on Communication and Signal Processing*, India, April 4–6, 2019.
6. Mondal, K., P. P. Sarkar, and D. C. Sarkar, "High gain triple band microstrip patch antenna for WLAN, Bluetooth and 5.8 GHz/ISM band applications," *Wireless Personal Communications*, Vol. 109, 2121–2131, 2019.
7. Yu, Z., Z. Lin, X. Ran, Y. Li, B. Liang, and X. Wang, "A novel "回" pane structure multiband microstrip antenna for 2G/3G/4G/5G/WLAN/navigation applications," Vol. 2021 — Article ID 5567417 — <https://doi.org/10.1155/2021/5567417>.
8. Goud, J. R., N. V. Koteswara Rao, and A. M. Prasad, "Design of triple band U-slot MIMO antenna for simultaneous uplink and downlink communications," *Progress In Electromagnetics Research C*, Vol. 106, 271–283, 2020.
9. Rajalakshmi, P. and N. Gunavathi, "Compact complementary folded triangle split ring resonator triband mobile handset planar antenna for voice and Wi-Fi applications," *Progress In Electromagnetics Research C*, Vol. 91, 253–264, 2019.
10. Saraswat, K. and A. R. Harish, "Flexible dual-band dual-polarised CPW-fed monopole antenna with discrete-frequency reconfigurability," *IET Microwaves, Antennas & Propagation*, Vol. 13, No. 12, 2053–2060, 2019.
11. Ali, T. and R. C. Biradar, "A triple-band highly miniaturized antenna for WiMAX/WLAN applications," *Microwave and optical Tech. Letters*, Vol. 60, No. 2, 466–471, 2018.
12. Bashir, U., K. R. Jha, G. Mishra, G. Singh, and S. K. Sharma, "Octahedron shaped linearly polarized antenna for multi-standard services including RFID and IoT," *IEEE Transactions on Antennas and Propagation*, Vol. 65, No. 7, July 2017.
13. Pandit, V. K. and A. R. Harish, "A compact CPW-fed triple band monopole antenna for WLAN/WiMAX applications," *Proceedings of the Asia-Pacific Microwave Conference*, 2016.
14. Fadamiro, A. O., J. D. Ntawangaheza, O. J. Famoriji, Z. Zhang, and F. Lin, "Design of a multiband hexagonal patch antenna for wireless communication systems," *IETE Journal of Research*, 2019.